



Glioblastoma Image Analysis using Convolutional Neural Networks to Accurately Classify Gene Methylation and Predict Drug Effectiveness

Glioblastoma multiforme is a deadly brain cancer with a median patient survival time of 18-24 months. A single biopsy cannot provide complete assessment of the tumor's microenvironment, making personalized care limited. 50% of the patients do not respond to the anti-cancer drug Temozolomide (TMZ) because of the over-expression of MGMT gene. Epigenetic silencing of the MGMT gene by methylation results in decreased MGMT expression, increased sensitivity to TMZ, and longer survival. The purpose of this research is to use artificial intelligence (AI) to design a low-cost platform to determine the MGMT's methylation status and suggest non-invasive treatment plan.

An AI platform is developed that uses a U-Net architecture for tumor identification in the brain MRI scans, and a ResNet-50 architecture for methylation prediction using MRI scans from the TCIA (The Cancer Imaging Archive) along with genetic data from TCGA (The Cancer Genome Atlas). The foundational software is written using Python, math libraries and TensorFlow.

Image segmentation of 5000 patient brain MRI scans using a U-Net model revealed an accuracy of 90% for tumor segmentation. ResNet50 image classifier model was used for MGMT methylation status prediction. The web- platform quickly uploads the MRI scans and provides MGMT status in few seconds. The platform allows oncologists to recommend personalized treatment plans, eliminating huge time/cost investments of invasive biopsies. Patients with Positive/methylated MGMT will be receptive to chemotherapy with TMZ. Patients with unmethylated MGMT will not be sensitive to TMZ and would need additional MGMT modulation with miRNAs.

Keywords: Glioblastoma ■ Anti-cancer ■ Brain MRI ■ Artificial intelligence ■ Cancer

Introduction

Glioblastoma multiforme is a very lethal form of brain cancer with no known cure. The prognosis remains poor with a 5% average survival rate, despite aggressive treatments. For high grade gliomas, treatment combines surgical resection, postoperative radiation, and chemotherapy using temozolomide (TMZ), an alkylating agent [1-3]. Although radiation therapy and chemotherapy with TMZ contribute to lengthen the survival and improve quality of life, the survival advantages are still palliative due to TMZ resistance as primary reason for GBM treatment failure [4-6], as 50% of TMZ treated patients do not respond to TMZ [7-9]. The methylation status of the O6-methylguanine-DNA methyltransferase (MGMT) gene promoter region impacts sensitivity to temozolomide by repairing the main cytotoxic lethal base pairs, which are composed of the alkylating agent TMZ, and hence, is linked to reliably predicting effectiveness of TMZ [9, 10].

MGMT is an enzyme involved in DNA dealkylation and mediation of DNA damage, and is overexpressed in 60% of glioblastomas [1,11]. MGMT encodes for a DNA repair enzyme that provides resistance to alkylating chemotherapies such as temozolomide (TMZ).

Because MGMT transcription can be silenced by promoter methylation in tumor cells, MGMT promoter methylation in patient tumors causes decreased MGMT protein expression, thereby abrogating the DNA repair activity necessary for TMZ resistance [2] (mechanism explained in the Figure 1). Thus, patients with a methylated MGMT promoter have improved survival and better response to radiation with concurrent temozolomide-based therapy. Hence, methylation of the O-6-methylguanine-DNA methyltransferase (MGMT) gene promoter has emerged as a strong prognostic factor for newly diagnosed glioblastoma [2] Figure 1.

MGMT is not a true enzyme since this active enzyme is not regenerated after it is alkylated (hence MGMT is also known as suicide enzyme).

The picture below shows survival rate for low risk and high-risk patients in 4 cases:

- 1) The survival improvement for patients with radio therapy (RT) using temozolomide.
- 2) Standard radiotherapy without temozolomide
- 3) Impact of RT+TMZ in case of unmethylated MGMT.
- 4) Impact of RT+TMZ in case of methylated MGMT [4] on the survival rate for low-risk

Viraj Mehta*

High school senior student, Basis
Scottsdale, Scottsdale, USA

*Author for correspondence :
Viraj28m@gmail.com

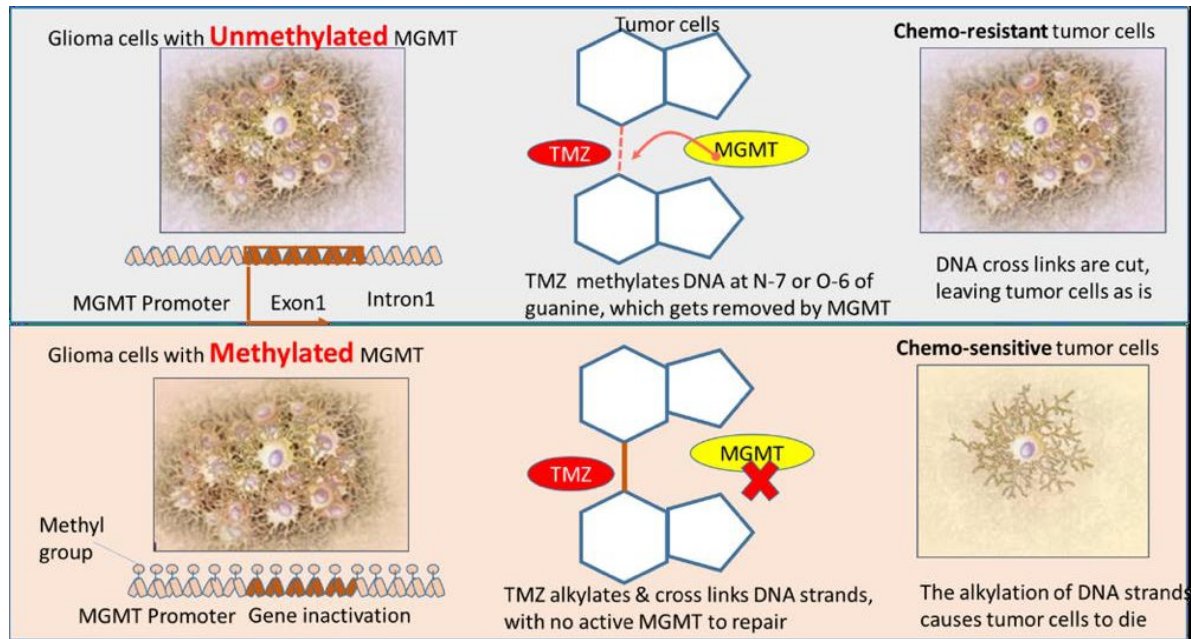


Figure 1. Chemosensitivity of MGMT: Enhanced due to epigenetic silencing of the DNA-repair gene MGMT [10 O⁶-alkyl-guanine is a major carcinogenic lesion in DNA. Above shows that the DNA adduct is removed by the repair protein MGMT (O⁶-alkylguanine DNA alkyl transferase).

and high-risk patients is shown below in Figure 2. Radiotherapy and TMZ combined confers a clear overall survival benefit to patients with methylated MGMT relative to standard radiotherapy [12] Figure 2.

Additionally, MGMT can be epigenetically repressed in multiple ways, most commonly due to methylation of its promoter region, or by over-expression of several microRNAs [7].

MicroRNAs are small noncoding RNAs that target specific sequences of mRNAs, thereby regulating gene expression, causing translational repression or mRNA degradation [7].

This is summarized in the following Table 1:

Problem statement: Current methods for tumor detection and MGMT gene methylation identification to recommend effective TMZ dosages to glioblastoma patients are extremely invasive and time- and cost- intensive. Current methods use invasive biopsies and expensive procedures like genetic testing that add to the financial burden and unnecessary time lag between patient testing and therapy recommendation [13-17].

Proposal: The combination of brain MRI scans, genetic data, and deep learning models can be used to detect microscopic changes in brain tumors and predict MGMT methylation status in a time- and cost- effective manner. In the current study, the author develops an AI

platform, that will facilitate efficient diagnoses by executing the following real-time analysis:

1. Perform tumor segmentation on the patients' brain MRI scans which are uploaded by clinicians. The background on this step includes algorithms that train a deep learning U-Net model on the BraTS dataset (Brain Tumor Segmentation) and then training a U-Net architecture on a TCIA database to perform tumor segmentation (predict tumor areas). Note that the TCIA database was used in this study as retrospective data for patient MRI scans.
2. Label patient scans with tumors clearly identified with known MGMT methylation status. This data was obtained retrospectively from TCGA datasets.
3. Train a convolutional neural network using the ResNet-50 model and the combined TCGA and TCIA data to predict MGMT methylation status and overall survival for patients with methylated and unmethylated MGMT.
4. Recommend therapeutic options (Radiotherapy (RT) + Chemotherapy with TMZ or only RT depending on MGMT methylation status).
5. Perform computation modeling using miRNA databases and MGMT interaction to find miRNAs that can regulate MGMT expression, leading to improved TMZ sensitivity for patients with unmethylated MGMT.

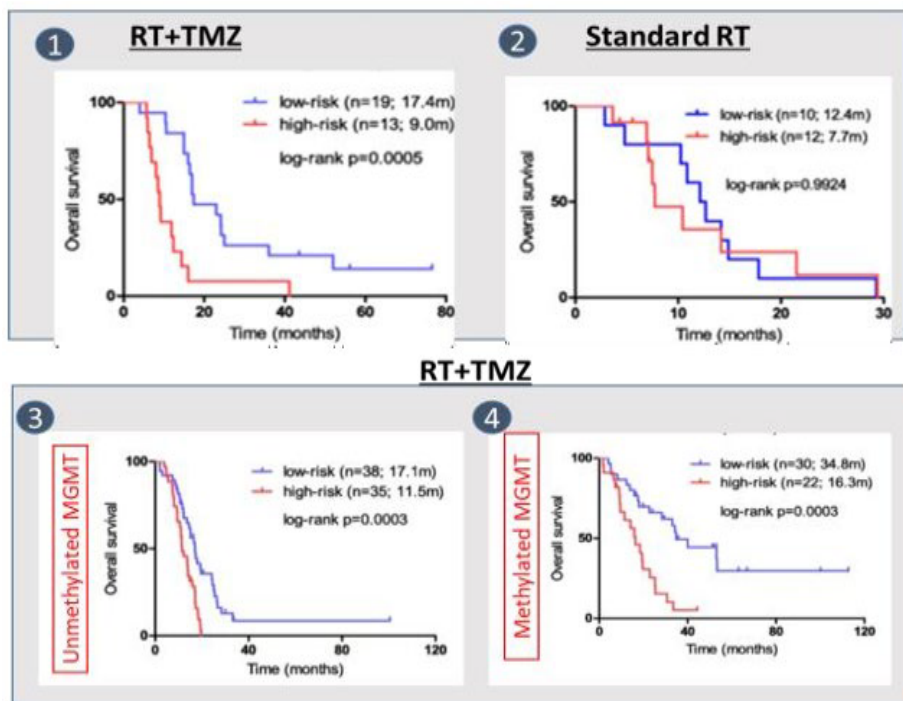


Figure 2. MGMT and Overall survival [12].

Table 1. This is summarized in the following table.

	Methylated MGMT	Unmethylated MGMT
What is it	CH3 or methyl group gets added	No CH3 or methyl addition
Why it happens	Environmental factors, genetic mutations	
Anti-cancer drug temozolomide (TMZ)	Works (glioma cells sensitive to TMZ)	Does not work (glioma cells resistant to TMZ)
Therapeutics for Glioma	Radiotherapy (RT) + TMZ	Radiotherapy only
Consequences	Improved patient survival	Reduced patient survival
Options for enhanced and improved treatment	Radiotherapy + TMZ (Temozolomide)	miRNA-based MGMT modulation to enhance sensitivity to TMZ

Essentially, miRNAs downregulate MGMT gene expression in GBM cells through binding to the 3'-UTR of MGMT mRNA, thereby affecting protein translation [18]. MiRNA transfection thus leads to significant improvement in responsiveness to TMZ, causing GBM cell death [18] Figure 3.

The overall architectural overview for this methodology is shown below in Figure 4:

Methods and Materials

Step 1: Download patient images from TCIA, shown below in Figure 5. 4,959 Brain Scans (475,458 image frames) for 259 patients were downloaded from TCIA with all 4 modalities (T1, T2, FLAIR, T1Gd). Only T1 image scans were used to keep uniformity, as all patients did not have T2/FLAIR/T1Gd.

Figure 5: Subset of 4,959 images downloaded from The Cancer Imaging Archive (TCIA)

Step 2: preprocessing of images: raw downloaded images needed to be processed into usable formats. Skull removal using BET (brain extraction tool) was performed, as well as noisy image analysis and axis correction. Figure 6.

Final Pre-processed Images Figure 7:

Step 3: Tumor segmentation using the U-Net Convolutional Neural Network Architecture

Training U-Net on the BraTS dataset (Images downloaded from medicaldecathlon.com). The BraTS (Brain Tumor Segmentation) dataset provides evaluation of state-of-the-art methods for the segmentation of intrinsically heterogeneous (in appearance, shape, and histology) brain tumors, namely gliomas [13]. A U-Net architecture was trained on the BraTS dataset to create a pixel-wise segmentation map that would predict the tumor region in a brain MRI scan. A U-Net Convolutional Neural Network contains an encoder path, which



Figure 3. miRNA based MGMT regulation.

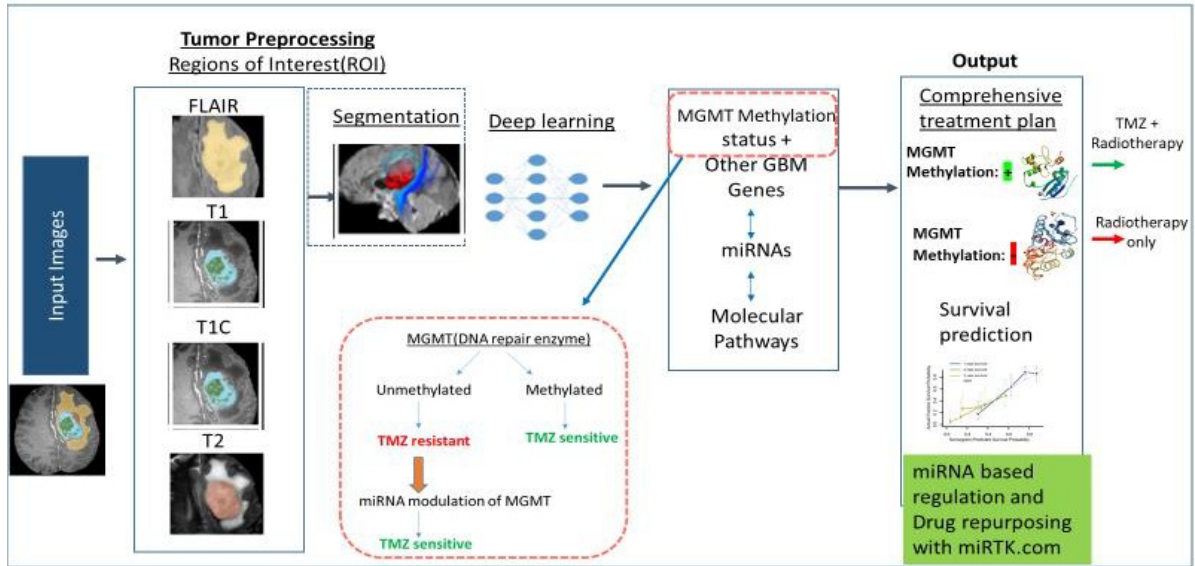


Figure 4. The workflow analysis approach used in this research.

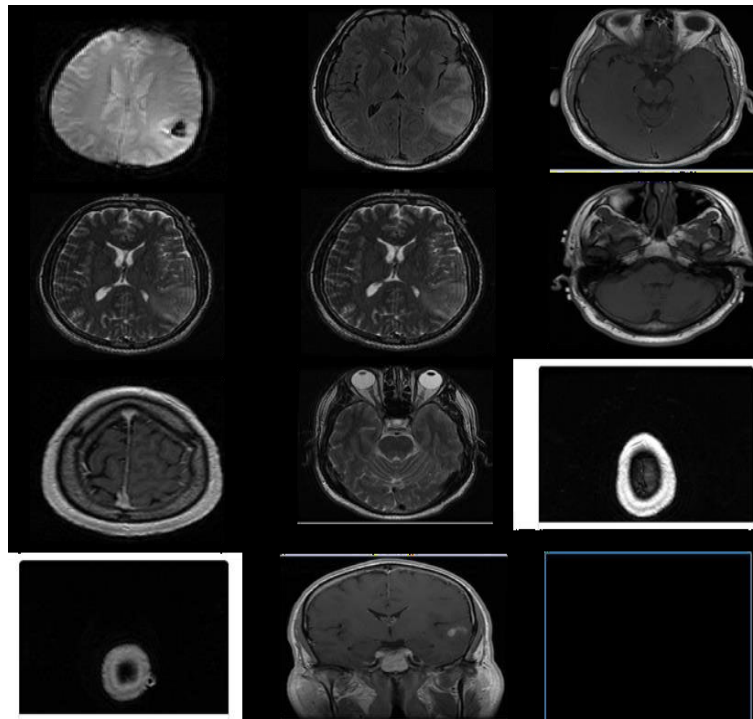


Figure 5. Subset of 4,959 images downloaded from The Cancer Imaging Archive (TCIA)

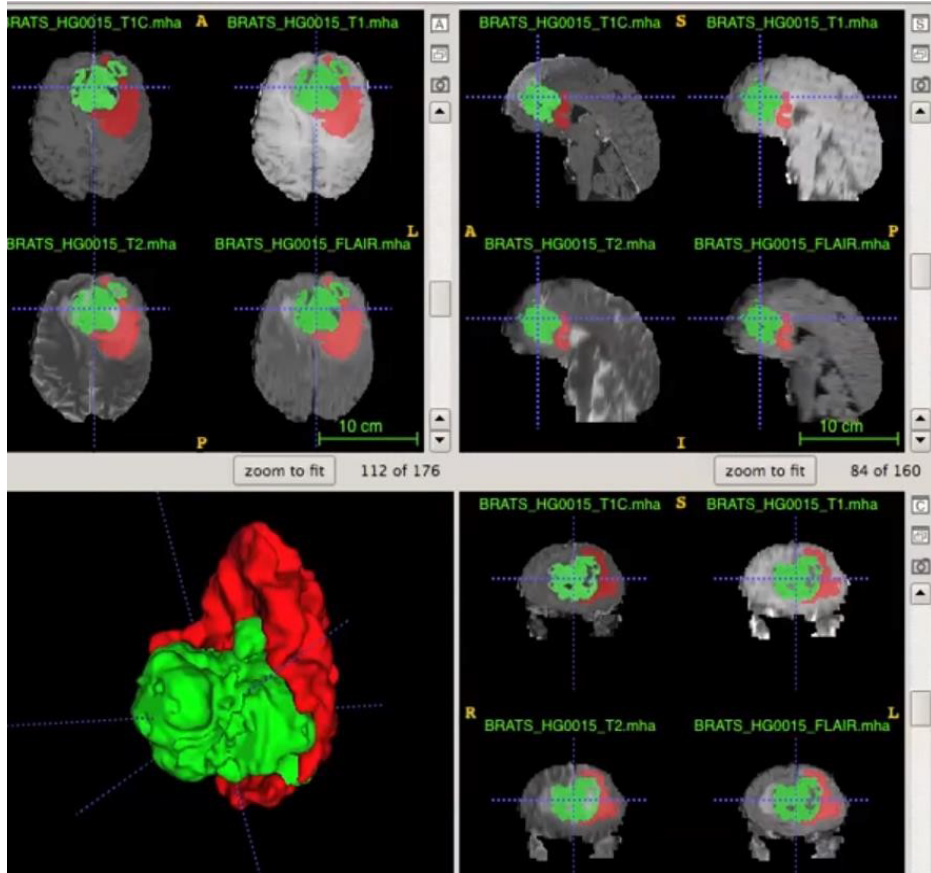


Figure 6. pre-processing using s/w tools

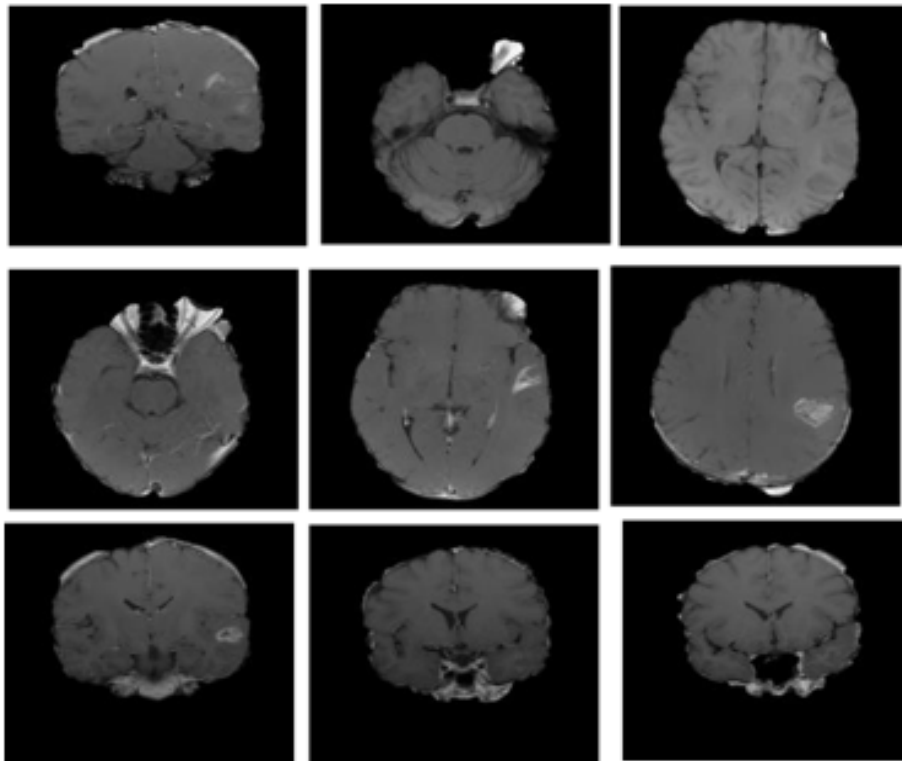


Figure 7. Subset of pre-processed images after skull removal, noisy image removal, and T2/FLAIR/T1Gd modality removal

reduces image dimensionality to capture the context of the image, and a decoder path, which enables precise localization using transposed convolutions and up-sampling [20-21] Figure 8.

Parameters used were as following:

The Sorenson-Dice coefficient was used to predict accuracy: the Sorensen–Dice coefficient is a statistic used for comparing the similarity of two samples, Figure 9 defined as

Dice (P,T) = $2|P \cap T| / (|P| + |T|)$, where P is algorithmic predictions $\in \{0,1\}$ and T is consensus truth $\in \{0,1\}$

True Negative also called Spec (P,T) = $|P \cap T^c| / |T^c|$

True Positive also called Sensitivity (P,T) = $|P \cap T| / |T|$

Ref: IEEE, The multimodal BraTS benchmark [13] The algorithm compares the UNet based predicted tumor location to the actual tumor location in the BraTS dataset.

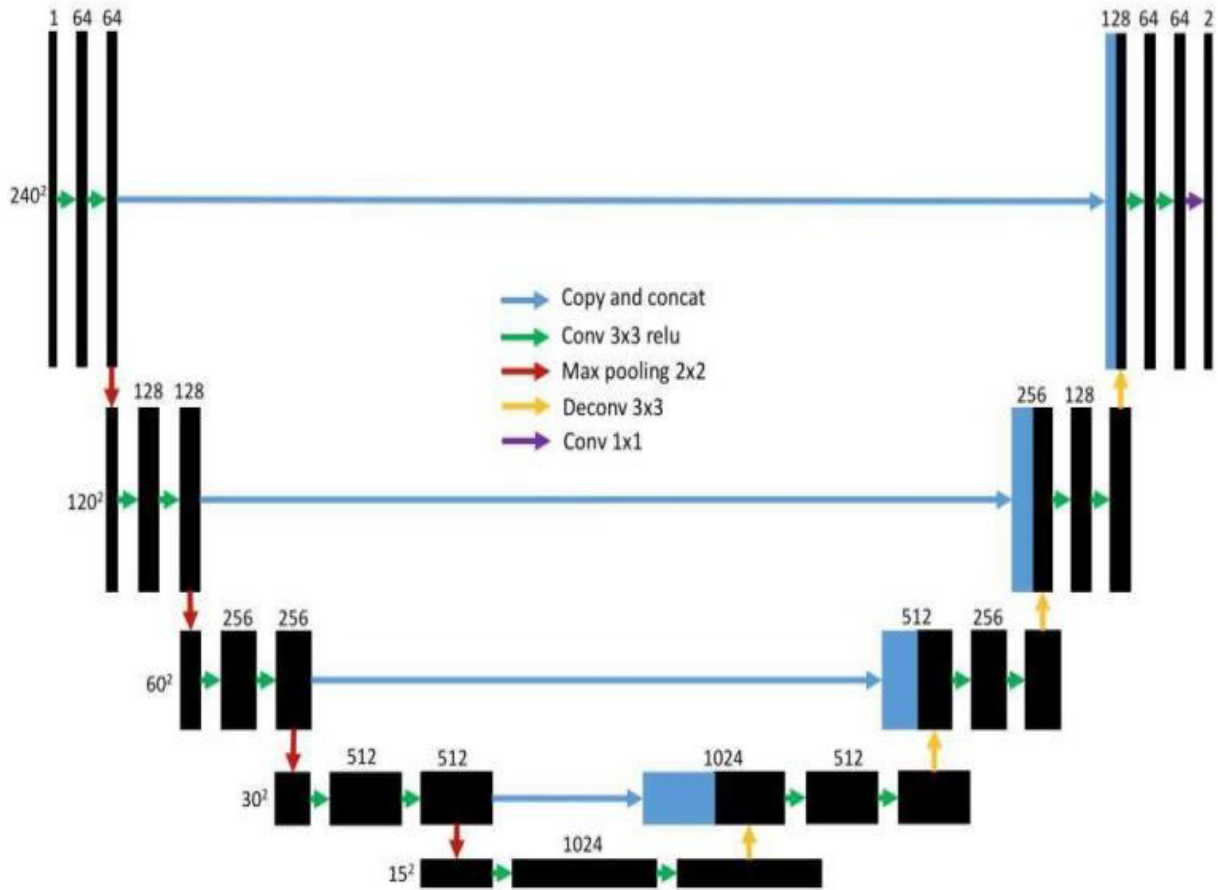


Figure 8. U-Net architecture showing the encoder and decoder path with input image, convolutional layers, max pooling, and final convolution calculated for the output image.

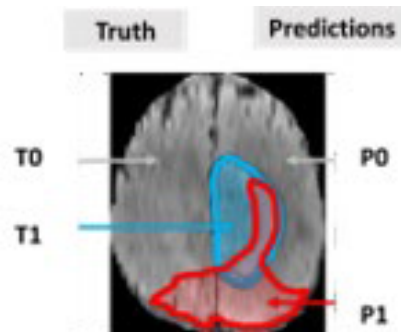


Figure 9. Sorenson-Dice coefficient.

Step 4: Genomics (methylation data) was retrieved from the TCGA website [3] and filtered by TCGA-GBM, DNA methylation, and methylation β value. The methylation consisted of 423 unique patients for all 450 methylation data files available on TCGA. Methylation sites (cg02941816, cg12434587, and cg12981137), located in the minimal promoter and enhancer regions, shown to have maximal methylation activity and affect MGMT expression, were extracted. Methylation values for these 3 mentioned sites were taken, and a patient was considered to have a positive MGMT methylation status if the maximum of the three was greater than 0.2 (i.e. a methylation beta value of minimum 0.2 was a positive methylation site). In general, the methylation value for each site is expressed as a β value, representing a continuous measurement from 0 (completely unmethylated) to 1 (completely methylated). Following the merge of the preprocessed T1 modality MRIs from the TCIA dataset with the methylation labels, the final patient count was:

The resulting methylation data was mapped to patient IDs and T1 images. The data was then used to train a second CNN to predict a patient’s methylation status using a ResNet-50 architecture Figure 10.

In general, in a deep convolutional neural network, several layers are stacked and trained

with labeled data. The network then learns features at various levels of abstraction (high/medium/low level). In residual learning, instead of trying to learn features directly, it tries to learn from a residual. ResNet-50 does this by using shortcut connections (directly connecting input of n th layer to some $(n + x)$ th layer [14]. It has been proven that training this form of networks is easier than training simple deep convolutional neural networks and the problem of “deterioration of training accuracy” is addressed to ensure a certain performance level [14].

The ResNet-50 classification model has 5 stages each with a Convolution and Identity block. Each convolution and identity block has 3 convolutional layers. Each image frame was first input in a CNN layer, and multiple residual convolutional layers were used to detect edges/shapes/corners that represent the tumor in the image. Batch normalization and average pooling layers were added to improve speed, and performance. Final dense layers were added with 2 nodes for classification (methylation positive or methylation negative).

Training set (80%) and Validation set (20%)

The area under the receiver operator characteristic curve (ROC), accuracy, and precision were all calculated.

Step 5: For patients with “unmethylated MGMT,” computational modeling was done

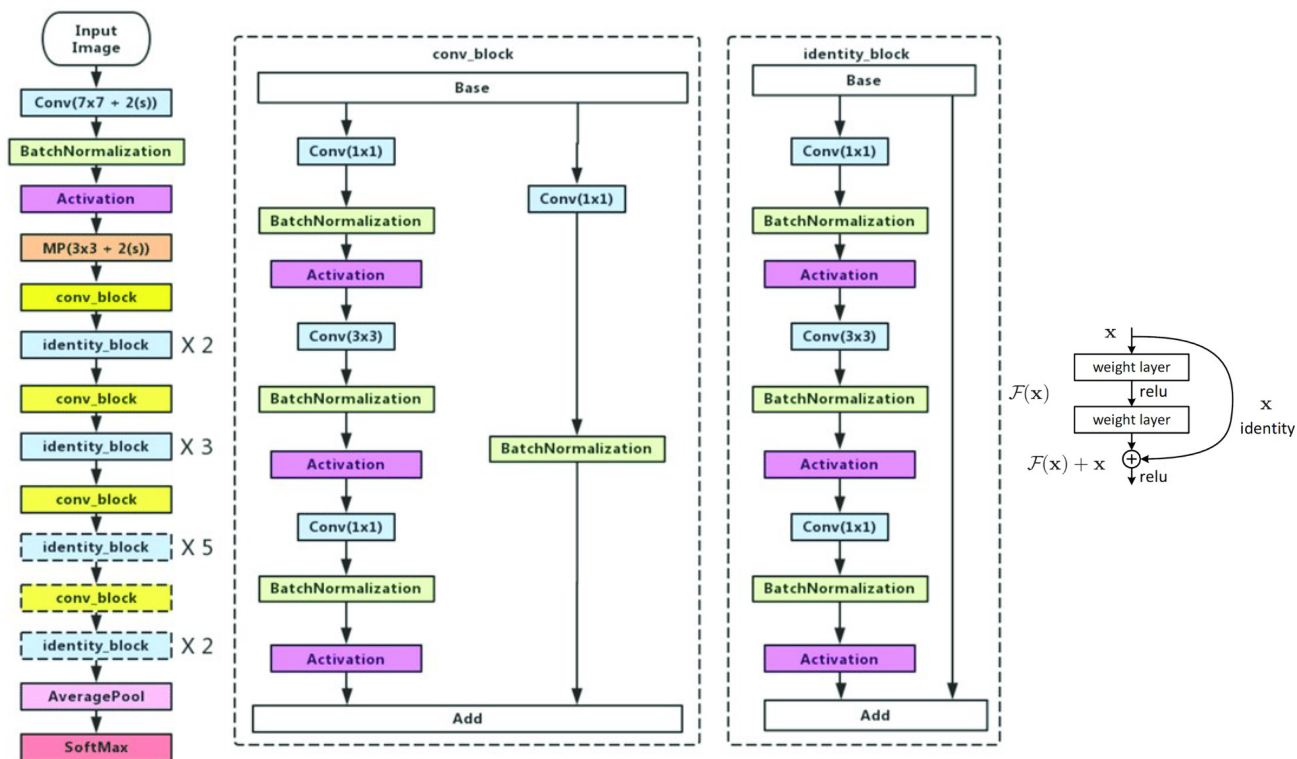


Figure 10. ResNet-50 CNN Architecture for state-of-the-art image classification.

to find miRNAs and binding strength with MGMT. Binding sites for miRNAs in the 3' UTR of MGMT were predicted using the tools TargetScan and miRTarbase. In addition, stronger miRNA-mediated repression of mRNA was observed with multiple binding sites for the same miRNA on 3'UTR. Table 2.

Results

Methylation status prediction accuracy

ResNet-50: Image Format: DICOM (Digital Imaging and Communications)

Initial Number of Patients: 259 (all modalities T1/T2/FLAIR), 475,458 images

Images with methylation status TRUE: 38,043; FALSE: 44,659

Number of epochs: 50

Training and Validation data split: 80%/20%

(Figure 11 & Figure 12)

The ROC Curve has an area under the curve of 0.93, demonstrating a high prediction accuracy for the validation set. The True Positive Rate (TPR), defined as the correctly predicted number of methylated patients out of the total number of

methylated patients, was 92.5%. The accuracy, defined as the correctly predicted number of patients out of the total number of patients (video-level accuracy), was 95%. Methylation results per frame were aggregated on a video level using a simple majority rules rule to get accuracy, true positive rate, and true negative rate numbers.

Overall survival: Kaplan Meier curve, drawn using Xenabrowser, demonstrates higher survival for patients with methylated MGMT vs unmethylated MGMT (drawn for a subset of the total dataset of patients) [15] Figure 13.

miRNA-MGMT mRNA analysis: In reference to Table 2, high absolute values of Minimum Free Energy and GSC (Geometric Share Complementarity Score) demonstrate the stability of the miR181d and miR603 binding. Thus, miR603 and miR181d can silence MGMT and improve glioma cell sensitivity to TMZ.

The regression analysis between miRNA and MGMT mRNA from the TCGA dataset indicated that miR-603 and miR-181d are consistently inversely related with MGMT mRNA in the TCGA dataset (p value of 0.005 and 0.006 respectively) Table 3.

Table 2. Paring between miRNA and 3' UTR of MGMT and Minimum Free Energy scores of the complex miR-181d and miR-603 ranked top 2 in "absolute" minimum free energy, pointing to these as miRNAs that can effectively regulate MGMT mRNA expressions. In addition, 3 of the 5 binding sites predicted for miR603 and miR-181d were within 40 nucleotides apart of each other, contributing to cooperative regulation of MGMT.

Gene = MGMT miRNA	Geometric Share Complementarity Score	Duplex structure	MFE kcal/mol (min free energy)
miR181d-5p	142	miRNA 3' ugggUGGCUGUUGUUACUACAA 5' : : : : : Target 5' taaaACAGGCCA-AGTGAGTGTg 3'	-20.9
miR767	139	miRNA 3' ucuuuGGUACCCCAUACUCGUcu 5' : Target 5' tggctTCAT---GTATGAGCAag 3'	-13.50
miR603	158	miRNA 3' ugCGCGU-CCGGUC---UCU----- GGGUCCGu 5' : : Target 5' ctGTCCAGGGCCAGCTAAGGCCCATCCC AGGCc 3'	-24.80
miR-409-3p	125	miRNA 3' uccCCAAGUGGCUC-- GUUGUAag 5' : : Target 5' caaGCTCTGCCGAGGCCGACATga 3'	-13.3
miR124-3p	135	miRNA 3' ccguaagUGGCG--CACGGAAu 5' : : Target 5' tgtgcgaGCCGCGAGTGCTTTc 3'	-15.6

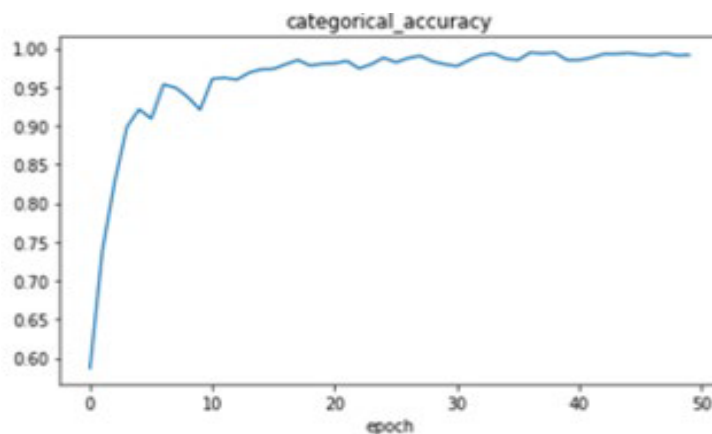


Figure 11. Training Accuracy.

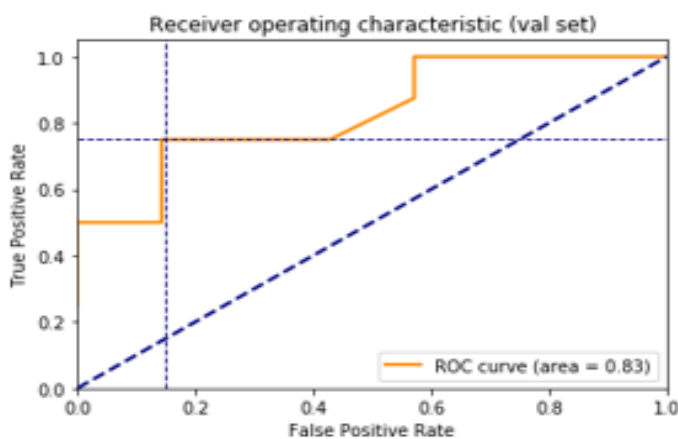


Figure 12. Images with methylation status.

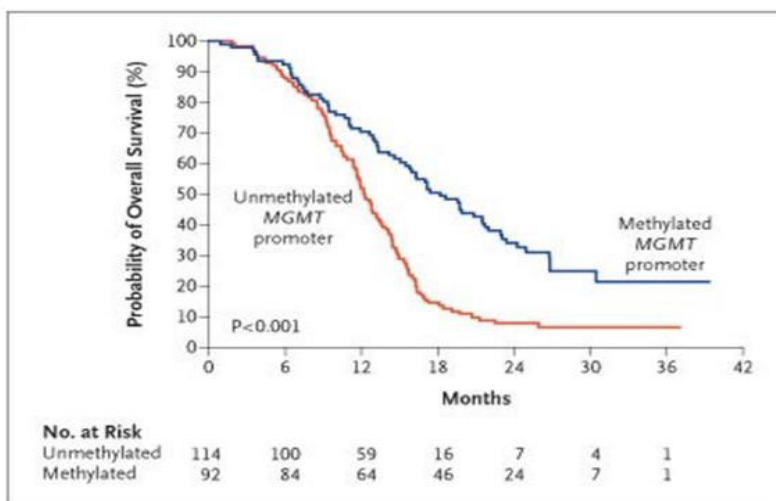


Figure 12. Images with methylation status.

Table 3. Correlation between MGMT mRNA (TCGA database) and miRNAs.

	miR-181d-5p	miR-603	miR-409-3p	miR-124-3p
r	-0.218	-0.211	0.073	-0.011
p-value	0.006	0.005	0.363	0.882

Discussion

The first CNN model used for tumor segmentation was a fully convolutional model with an encoder-decoder architecture (U-Net). The U-Net consists of 4 down-sampling blocks, in which the input image is scaled down using convolutional layers, followed by 4 up-sampling blocks in which the input image is scaled up using transpose convolution blocks.

The final loss, as measured by the dice loss coefficient, was 0.98 on the training dataset and 0.7 on the validation dataset. The dice loss (DL) is the intersection over union in which the intersection is factored in twice in the numerator and denominator [16].

Mathematically:

$$DL = 2TP / (2TP + FP + FN) = 2|X \cap Y| / (|X| + |Y|) \quad [16]$$

The second CNN, a classification model with a ResNet-50 backbone for MGMT methylation prediction was a convolutional network with two fully connected layers at the end to classify each image into one of two categories, methylated or unmethylated. A ResNet-50 has residual connections that enable an easier propagation of the error into the lower layers of the network. The input images to this model are individual frames of size 128x128x1 and an Adam Optimizer was also used with a learning rate of 0.0001, a batch size of 16, and 50 epochs. Additionally, the loss used was a categorical cross entropy loss with a categorical cross entropy accuracy for evaluation [17].

Categorical cross-entropy loss is defined as

2

$$CCE = - \sum_{i=1}^2 t_i * \log(f(s_i)) = -t_1 * \log(f(s_1)) - (1 - t_1) * \log(1 - f(s_1))$$

$i=1$

where $i=1$ if methylation is false, $i=2$ if methylation is true, $f(s_i)$: probability output for class i

t_i : 1 for true ground truth class, 0 otherwise. Simply put, it is the (negative) log of the probability output for the ground truth class [17].

The dataset used here for both training and validation was the TCIA dataset. Before dividing the dataset into a training and validation set, the trained segmentation model was used to identify frames in each video where the tumor was visible. If the BraTS dataset segmentation model didn't predict a tumor to be present on a

given frame of a video, that frame was not used for training or validation.

Using this approach, the accuracy on the training set was 99% and the accuracy on the validation set was initially 90%, as determined by the categorical cross entropy averaged over all data points. A dropout of 20% was used to avoid a possibility of overfitting. After aggregating the results on a video level and using a majority rules approach, the validation accuracy increased to a final accuracy of 95% using a threshold of 0.5. Additionally, analysis of the final ROC and accuracy curves show that at a 0.5 threshold the accuracy is maximized with a true positive rate of 92.5% and true negative rate of 97.5%.

Conclusion

Gene methylation is a control mechanism that regulates gene expression. MGMT is a DNA repair enzyme that causes resistance to the effect of alkylating chemotherapy. Aberrant methylation deactivates the gene, leading to loss of MGMT protein expression and reduced proficiency to repair DNA damage induced by alkylating chemotherapeutic agents, thereby increasing tumor susceptibility to alkylating agent-based chemotherapy [8]. Thus, MGMT methylation results in a favorable response to temozolomide, while an unmethylated or overexpressed MGMT reduces the efficacy of alkylating drugs and confers resistance to the TMZ treatment [10]. Hence, detecting expression levels of MGMT gene becomes crucial to narrow the options of alkylating agents (e.g. TMZ) or to select patients directly for a second line personalized therapy.

Since miRNAs regulate a variety of cellular processes, such as cell differentiation, cell proliferation, apoptosis, stress resistance and stem cell maintenance [18], they were a key part of this research to understand the posttranscriptional regulation of onco- or tumor-suppressor genes, and specifically MGMT. The author used computational models to predict miRNAs to regulate the MGMT expression and improve sensitivity to temozolomide to increase the overall patient survival rate. Of multiple miRNAs simulated, the MFE scores and geometric share complementarity scores (GSC) demonstrated miR603 and miR181d to bind with the 3' UTR of MGMT to suppress its expression. These 2 miRNAs (miR603 and miR-181d) were identified to suppress MGMT expression through binding to the 3'-UTR of MGMT mRNA, thus affecting its protein

translation. This leads to the conclusion that transfection of miR603 and miR-181d mimics into GBM cells can suppress MGMT mRNA and protein expression and sensitize GBM cells to the alkylating drug like temozolomide for patients with MGMT promoter unmethylated glioblastomas.

The platform provides a user-friendly interface backed by complex algorithms to perform real-time image processing, BraTS-based image segmentation, tumor cropping, and methylation status prediction of patient image scans within seconds, in contrast to traditional methods that take 7-10 days and are time and cost intensive.

Declarations

■ Funding

No external funding was received. All funds used towards developing the software were personal funds.

Data Availability

A subset of the imaging data, genetic data, neural network architecture, results, miRNA-MGMT regression analysis is shared in the research report as well as in the supplementary material section below.

Code Availability

The software algorithms perform the functions of download of retrospective data from TCIA and TCGA, preprocessing of images, removal of noisy images, skull removal, creating a subset of T1 images out of T1/T2/FLAIR, tumor identification using U-Net on BRaTS data, U-Net on TCIA, Image classification for methylation prediction on TCIA+TCGA datasets using ResNet50 arch. The code is

available on github.com and can be provided upon request sent to viraj28m@gmail.com

Authors' contribution

Development of software algorithms using Python and TensorFlow, to create deep learning U-Net and ResNet50 architecture for training and validating the imaging and genetic patient dataset, as well as creating web platform. Different software modules contributed by the author are:

- Exploratory_analysis.ipynb
- Custom_metrics.py
- Subset_t1_t2_flair.ipynb
- Predict_brats.ipynb
- Preprocess_func.py
- Preprocess_tcga_gbm.ipynb
- Segmentation_unet_explore.ipynb
- Tumor_unet_seg.ipynb
- Methylation_training.ipynb

Conflict of interest

None. It is hereby declared that there are no competing or conflict of interest.

■ Ethics Approval

This research study was conducted retrospectively from data publicly available on TCIA (The cancer imaging archive) and TCGA (The cancer genome atlas) and no ethical approval is required.

■ Compliance with ethical standards

There is no conflict of interests. Research uses open access data in public domain from TCGA (The Cancer genome atlas) and TCI (The cancer imaging archive).

REFERENCES

1. Chow D, Chang P, Weinberg BD *et al.* Imaging Genetic Heterogeneity in Glioblastoma and Other Glial Tumors: Review of Current Methods and Future Directions. *Am. J. Roentgenol.* 210, 30-38, (2018).
2. Brandes, Alba A *et al.* Role of MGMT Methylation Status at Time of Diagnosis and Recurrence for Patients with Glioblastoma: Clinical Implications. *Oncologist.* 22,432-437, (2017).
3. GDC. (n.d.). <https://portal.gdc.cancer.gov/>
4. Sang Y Lee. Temozolomide Resistance in Glioblastoma Multiforme. *Genes Dis.* 3, 198–210, (2016).
5. Chang P *et al.* “Deep-Learning Convolutional Neural Networks Accurately Classify Genetic Mutations in Gliomas.” *Am. J. Neuroradiology.* 39, 1201-1207, (2018).
6. Hegi ME, Diserens AC, Gorlia T *et al.* “MGMT Gene Silencing and Benefit from Temozolomide in Glioblastoma. *New. Eng. J. Med.* (2005).
7. Cabrini G, Fabbri E, Nigro CL *et al.* “Regulation of Expression of O6-Methylguanine-DNA Methyltransferase and the Treatment of Glioblastoma. *Int. J. Oncology.* 417-428, (2015).
8. Coverage Policies and Guidelines. Medical Policy Manual | BlueCross BlueShield of Tennessee, <http://www.bcbst.com/providers/coverage-policies-guidelines/index.page>.
9. Shabierjiang J, Takuya F *et al.* Potential Strategies Overcoming the Temozolomide Resistance for Glioblastoma. *Neurol. Med. Chir.* 58, 405–421, (2018).
10. Esteller M, Foncillas JG, Andion E *et al.* “Inactivation of the DNA-Repair Gene MGMT and the Clinical Response of Gliomas to Alkylating Agents. *New. Eng. J. Med.* (2000).
11. MGMT O-6-Methylguanine-DNA Methyltransferase [Homo Sapiens (Human)]

- Gene - NCBI. National Center for Biotechnology Information, U.S. National Library of Medicine. (2020).
12. Yin A, He Y, Etcheverry A *et al.* Novel predictive epigenetic signature for temozolomide in non-G-CIMP glioblastomas. *Clinical Epigenetics*. (2019).
13. Menze BH, Jakab A, Bauer S *et al.* The Multimodal Brain Tumor Image Segmentation Benchmark (BRATS). *IEEE Trans Med Imaging*. 34, 1993-2024, (2015).
14. He K, Zhang X, Ren S *et al.* Deep Residual Learning for Image Recognition. (2020).
15. Xenabrowser. (n.d.). <https://xena.ucsc.edu/>
16. Taha AA, Hanbury A. Metrics for evaluating 3D medical image segmentation: Analysis, selection, and tool. *BMC Med Imaging*. (2015).
17. Brownlee J. A. Gentle Introduction to Cross-Entropy for Machine Learning. (2019).
18. Si W, Shen J, Zheng H *et al.* The role and mechanisms of action of microRNAs in cancer drug resistance. (2019).
19. Joshua B, Robert P. Hounsfield Scale. (2011).
20. U-Net. (n.d.). <http://deeplearning.net/tutorial/unet.html>
21. Ahmad A, Nay S, O'Connor T. Direct Reversal Repair in Mammalian Cells. (2015).